

# 7 Viscoelastic Characterisation of Rubber Compounds

## 7.1 Introduction

The viscoelasticity of a compound is intimately related to its processability in the post-mixing operation such as extrusion and injection moulding. In this chapter, however, viscoelasticity is used to characterise the end-product of mixing. One area of importance is to relate the viscoelastic properties to the composition of the compounds. Because the rubber formulation usually contains many additives, only the additives which have a significant influence on mixing and on viscoelastic properties of the compound are discussed. This narrows down the material variables to rubber grades and fillers. The low MW additives such as extending oils, plasticisers and tackifiers are important but are not included here except for an example of the oil-extended rubber. All the compounds were mixed to give a satisfactory degree of homogeneity, judged to be acceptable on the basis of commercial standards.

## 7.2 Viscoelastic properties of compounds

The mechanical properties pertinent to the mixing of rubber include viscoelastic properties at small as well as large deformation and failure behaviour. An overriding question is how the viscoelastic properties of gum rubber contribute to these properties of the compounds. This question is answered by choosing several grades of gum rubbers which have the same chemical composition but are different in molecular architecture and therefore, have different viscoelastic properties. Selecting a standard formulation which gives satisfactory mixing, the viscoelastic properties of gum rubbers and compounds may be compared. Samples for this experiment were NBRs with 33% acrylonitrile content [1] (see Table 7.1).

The characterisation of gum rubber is discussed extensively in Chapter 6 and reference [2]. Samples A and B are gel-free if analysed using ASTM D3616-95 [3]. The main difference is in the Mooney index [4]. Samples B, C, and D have similar Mooney values but their viscoelastic properties are very different from each other. Sample C contains 50% microgel, crosslinked particles, whereas Sample D has 75% macrogel, a molecule having many long branches. The compounds contain 40 phr N550 carbon black.

Table 7.1 Butadiene-acrylonitrile Copolymer Samples				
Sample code for filled elastomer	Sample code for raw elastomer	Raw elastomer Hycar <sup>a</sup>	T <sub>g</sub> (°C)	Mooney (ML-4) at 100 °C
1	A	1052-30	-37, -24	35
2	B	1042	-36, -24	78
3	C	1042X82	-34, -24	81
4	D	1002	-28	85

Stress relaxation, capillary extrusion, dynamic and tensile stress-strain were measured [1]. The results of stress relaxation are presented in Figure 7.1a for the gum rubbers and Figure 7.1b for the compounds.

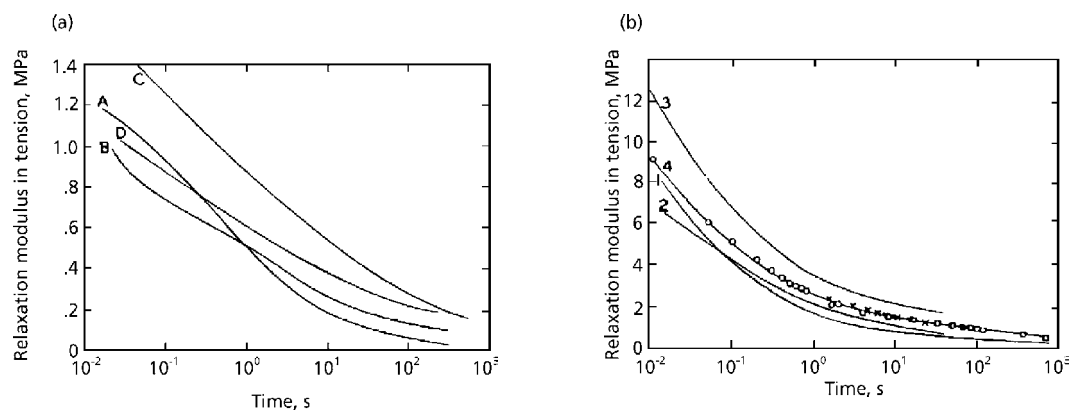


Figure 7.1 (a) Stress relaxation curves, reduced to 25 °C, of unfilled elastomers.  
 (b) Stress relaxation curves, reduced to 25 °C, of four carbon black filled elastomers.  
 25 °C (O) ; 54→25 °C ( x ); 98.5→25 °C (□).

Reprinted from N. Nakajima, *Polymer International*, 1996, 40, 2, 141. Copyright 1996, SCI.  
 Reproduced with permission.

The capillary extrusion data [5] are shown in Figures 7.2a and 7.2b. As seen in these figures, the relative differences between the gum rubbers remain in the filled compounds. Moreover, the magnitudes of the differences are not diminished in the presence of carbon black.

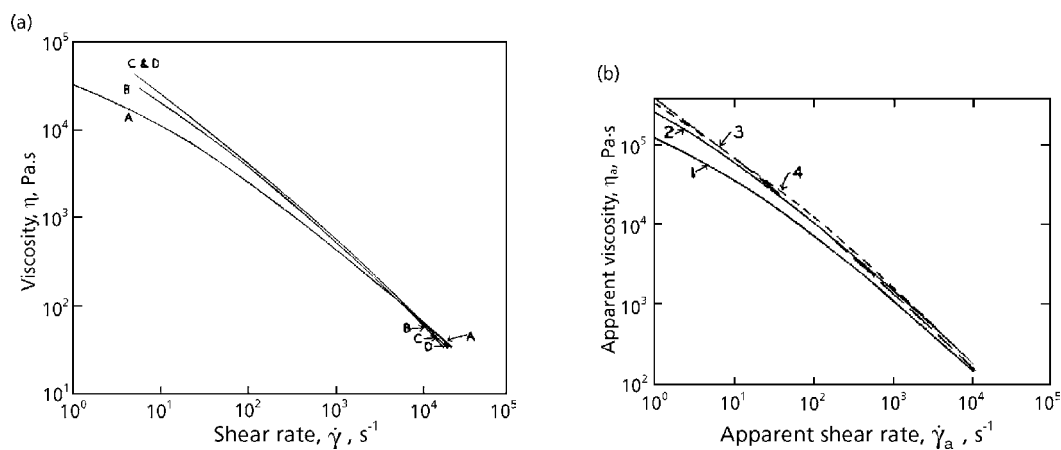


Figure 7.2 (a) Steady shear flow curves, reduced to 100 °C, of unfilled elastomers.  
(b) Steady shear flow curves, reduced to 100 °C, of carbon black filled elastomers.

*Reprinted from N. Nakajima, Polymer International, 1996, 40, 2, 141. Copyright 1996, SCI.  
Reproduced with permission.*

In Figure 7.3 the tensile strength and the strain at break for the gum rubbers are shown as functions of strain rate. Each gum rubber has its own unique behaviour. The locus of tensile strength and strain at break is known as the failure envelope, which is a characteristic for a given rubber [6]. The failure envelope is in turn related to the mill processability of the gum rubber, as explained in Chapter 2 and [7].

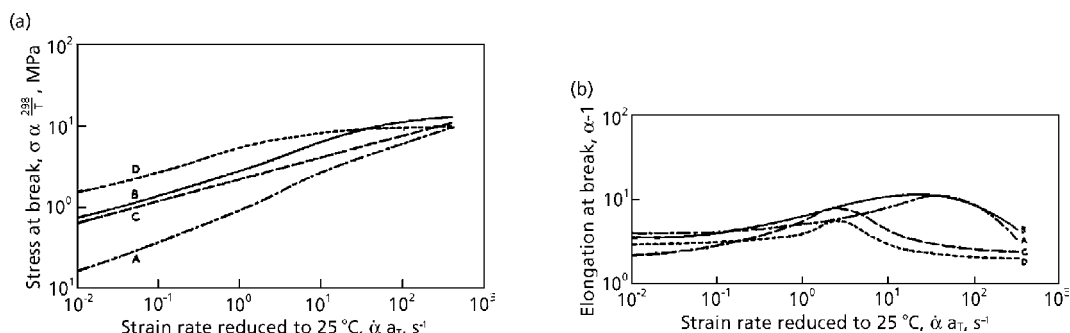


Figure 7.3 (a) Stress at break as a function of strain rate, reduced to 25 °C, of unfilled elastomers.

(b) Elongation at break as a function of strain rate, reduced to 25 °C, of unfilled elastomers.

Reprinted from N. Nakajima, *Polymer International*, 1996, 40, 2, 141. Copyright 1996, SCI. Reproduced with permission.

The tensile strengths of the compounds are shown in Figure 7.4a, where the relative differences among the gum rubbers are more or less retained. However, some parts of the curves are not exactly in the same order as those of the gum rubbers. Also, at higher strain rates the differences between the samples becomes very small.

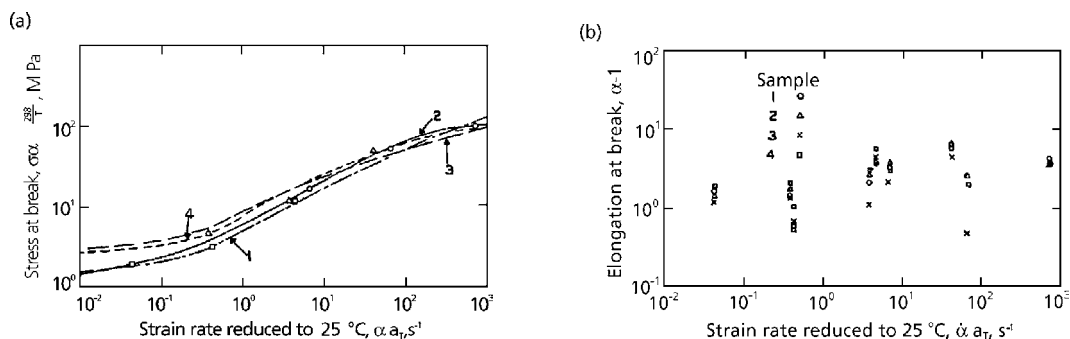


Figure 7.4 (a) Stress at break as a function of strain rate, reduced to 25 °C, of carbon black filled elastomers. 25 °C (O), 56→25 °C ( $\Delta$ ), 98.5→25 °C ( $\square$ ).

(b) Elongation at break as a function of strain rate, reduced to 25 °C, of carbon black filled elastomers.

Reprinted from N. Nakajima, *Polymer International*, 1996, 40, 2, 141. Copyright 1996, SCI. Reproduced with permission.

The strain at break (Figure 7.4b) shows no difference among samples, nor any specific pattern. Fracture of gum rubber during mixing has been discussed in Chapter 4. The compounds consist of mixtures of carbon black and comminuted rubber particles. The tensile strength and tensile strain at break depend largely on the strength of cohesion between the rubber particles and the extent of recovery of entanglement in the interparticle boundary. They must also depend upon the growth of the bound rubber. These mechanisms may exert an overriding influence on the tensile strength and the differences among the gum rubbers become secondary. Considering that fracture is initiated from flaws in the material, there must be a wide distribution of flaws in the compounds so that the strain at break data are scattered at random. Why the stress at break data are not scattered is an unanswered question.

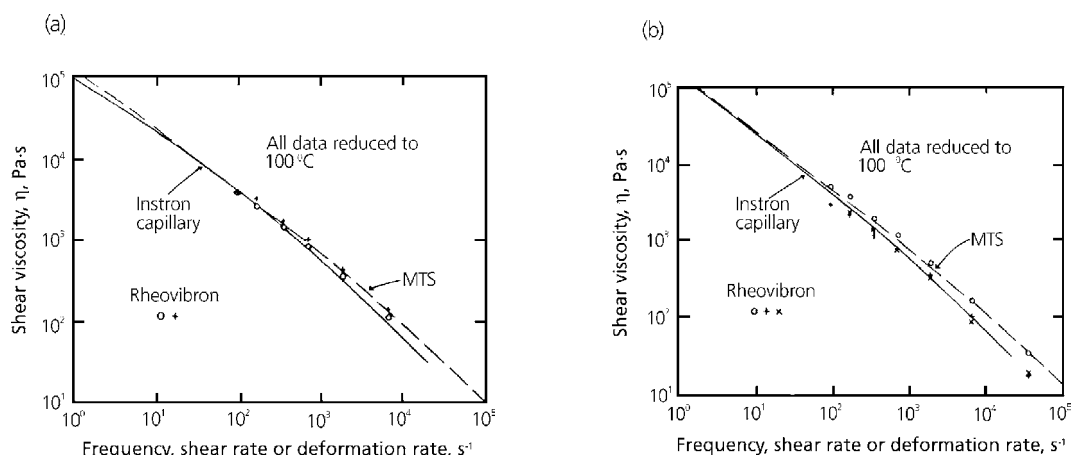


Figure 7.5 (a) Viscosities of gum rubber B obtained by capillary extrusion, dynamic oscillatory and tensile stress-strain measurements.  
(b) Viscosities of gum rubber C obtained by capillary extrusion, dynamic oscillatory and tensile stress-strain measurements.

Reprinted from N. Nakajima, *Polymer International*, 1996, 40, 2, 141. Copyright 1996, SCI. Reproduced with permission.

In Figures 7.5a and 7.5b the tensile stress-strain, dynamic and capillary extrusion data are compared for samples B and C, respectively. The tensile data obtained using a High Speed Tension Tester (MTS Systems), are linearised according to the method described in Chapter 6 and [2, 7], i.e., strain-time correspondence. The results are presented as the equivalent of shear viscosity. The results obtained show good agreement with the dynamic data (Rheovibron) within the reproducibility of the experiments. The steady state viscosities from capillary extrusion are also in approximate agreement, and the Cox-Merz empirical rule is applicable in these cases [8].

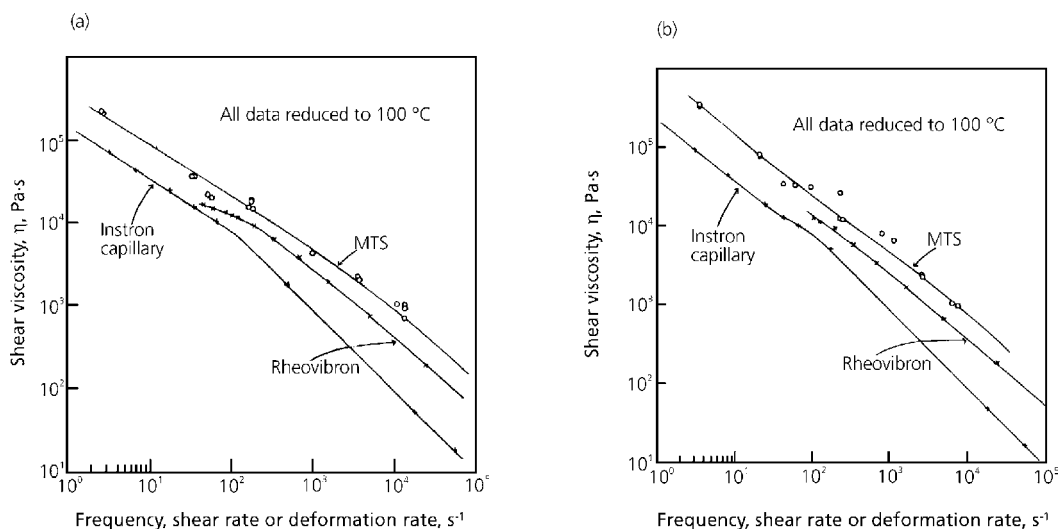


Figure 7.6 a) Viscosities of compound 2 obtained by capillary extrusion, dynamic oscillatory and tensile stress-strain measurements.  
b) Viscosities of compound 3 obtained by capillary extrusion, dynamic oscillatory and tensile stress-strain measurements.

Reprinted from N. Nakajima, *Polymer International*, 1996, 40, 2, 141. Copyright 1996, SCI. Reproduced with permission.

The result for the compounds from the same sets of the experiments are shown in Figures 7.6a and 7.6b. The viscosities evaluated through the three different experiments differ significantly.

The reason for this lies in the fact that it is a dispersed system. The dispersed carbon black is a complex-shaped fine particle, which is hard and not deformable. The matrix rubber is soft and easily gives a large deformation. Also, the dispersed carbon black usually forms a network consisting of strings of particles. The network crumbles easily upon deformation, resulting in a decrease of modulus [9]. Moreover, a part of the rubber is adsorbed on the surface of the carbon black, forming bound rubber, which does not dissolve in solvent. The amount of bound rubber may be as much as 25%. When the temperature is raised, more rubber is extracted and at certain elevated temperatures all the rubber dissolves [10, 11]. In summary the compound consists of carbon black, bound rubber and unbound rubber; each component responds differently at small deformations (Rheovibron) and large deformations (MTS), and with shear (capillary) and elongation (Rheovibron and MTS).

Even though the viscoelastic behaviour is complex, characterisation methods may be developed for relatively easy interpretation. One is the dynamic shear measurement, which provides storage modulus and loss modulus as functions of angular frequency. Because the behaviour of compounds is strain-dependent, the strain amplitude must be kept at a constant value for all samples.

The tensile stress-strain measurements are conducted at different strain rates [12]. These characterisation methods are the same as those for gum rubbers [2]. The tensile data for five different strain rates are shown to form a master curve upon application of the strain-time correspondence, which requires modification of the observed time by multiplying by the extension ratio,  $\alpha$  (see Figure 7.7). This conclusion is the same as the case for gum rubbers [2, 7]. However, an important difference of the compound behaviour is the yielding which does not occur in gum rubbers. Therefore, the data up to the yield point are used for the master curve. The data after yielding are inaccurate because deformation often becomes non-uniform.

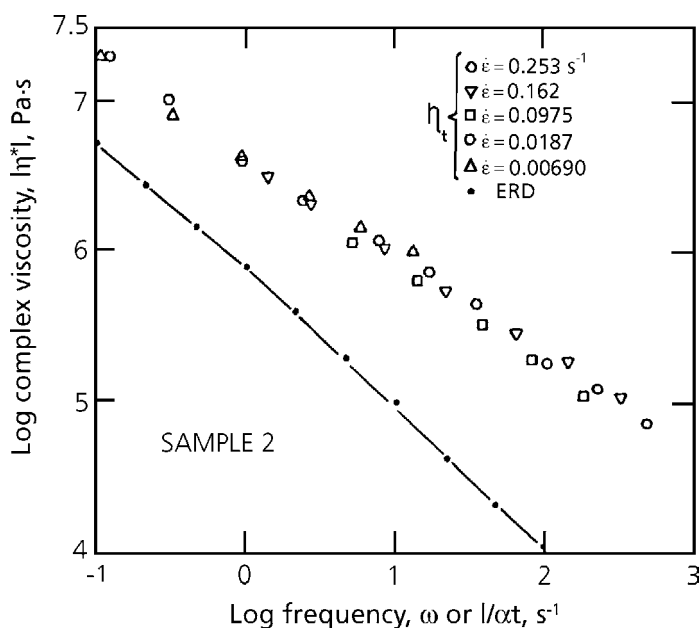


Figure 7.7 Tensile stress-strain data reduced to a master curve compared with dynamic shear data for Sample 2.

Reprinted from N. Nakajima, *Polymer International*, 1996, 40, 2, 141. Copyright 1996, SCI. Reproduced with permission.

The master curve obtained from the tensile data is compared with the curve obtained from dynamic shear measurements in Figure 7.7.

Unlike the gum rubbers, these two curves are in disagreement. Because Poisson's ratio of the compound is not 0.5, the disagreement is expected. However, the shear viscosity calculated from tensile data with the use of the factor 3 is about one order of magnitude higher than that of the dynamic shear data; hence Poisson's ratio alone does not provide the explanation for the disagreement, see Figure 7.7. The following is the explanation for the difference in the internal mechanism of deformation in tension and shear. When a test piece is elongated to twice its original length, it contracts by  $\sqrt{2}$  in the crosswise direction, if the volume change is negligible. If the affine deformation (the same deformation at both macroscopic and molecular scale) is assumed, this change of the dimensions must be valid even at the molecular level. However, the affine assumption brings the following contradiction [12, 13]. Figure 7.8 illustrates the elongation in a two-dimensional model, where the short lines may be assumed to be the molecules.

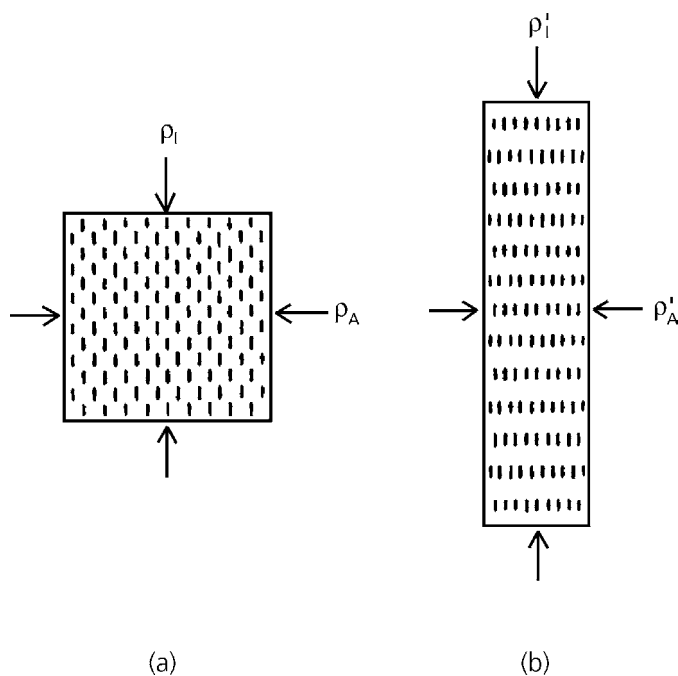


Figure 7.8 Hypothetical model of filled rubber: a) before elongation; b) during elongation.

*Reprinted from N. Nakajima, Polymer International, 1996, 40, 2, 141. Copyright 1996, SCI. Reproduced with permission.*



For an extension ratio of 2 (Figure 7.8b), the density of molecules in the stretch direction,  $\rho_1'$  and that before stretching,  $\rho_1$  are related as

$$\rho_1' = \rho_1/2 \quad (7.1)$$

and the density in the cross-direction is given by

$$\rho_A' = 2\rho_A \quad (7.2)$$

In reality the compression in the cross-direction to a half width is impossible. This contradiction does not occur with gum rubbers, because of the liquid-like motion of the chain segments shorter than  $Me$ ; and consequently density rearrangement maintains isotropic density:

$$\rho_1 = \rho_A = \rho_1' = \rho_A' \quad (7.3)$$

The density rearrangement requires additional energy over the thermal motion but it is negligibly small.

With regard to the behaviour of compounds, the short lines in Figure 7.8 represent carbon black with adhered rubber. The size of these particles is about 100 nm, and they are not in a liquid-like motion. Therefore, the density rearrangement must occur through the considerable internal movement which is much larger than the macroscopically imposed deformation.

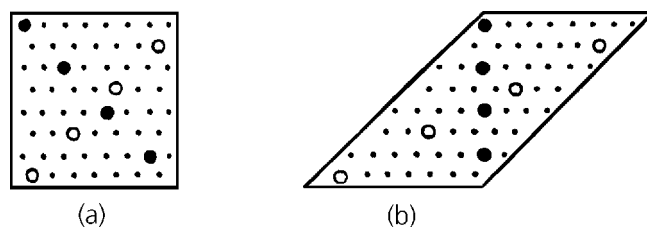


Figure 7.9 Hypothetical model of filled rubber: a) before shear; b) during shear.

*Reprinted from N. Nakajima, Polymer International, 1996, 40, 2, 141. Copyright 1996, SCI. Reproduced with permission.*

On the other hand, in shear deformation (Figure 7.9), the internal deformation requires little density rearrangement, because it is like the sliding of a deck of cards. The density

rearrangement in the direction of the black dots (contraction) and that in the direction of the white dots (expansion) may be insignificant. This explains the disagreement in Figure 7.7 between the complex viscosity calculated from tensile data and the shear viscosity.

### **7.3 Strain- and strain-rate amplification**

The nonlinear viscoelasticity modulus  $E(t, \epsilon)$  is a function of time,  $t$  and strain,  $\epsilon$ . The compound behaviour is nonlinear even at very small deformation [9]. As described in Chapter 6, the presentation of modulus data requires  $t$  and  $\epsilon$  axes. The plot is a curved surface. When we consider the property changes resulting from physical ageing and from various deformational history [14], the separability of time and strain does not hold and linearisation of nonlinear data will not work.

The complicated nature of the viscoelastic properties of compounds arises from three contributions. The first is the matrix rubber; the second is the carbon black, with its structure, spatial arrangement and self-interaction, and the third is the interaction between the rubber and the carbon black, including the bound rubber [15]. These three contributions each have a different temperature dependence and a different response to deformation.

In order to simplify the characterisation of the compounds a pragmatic approach is adopted. The following questions represent some of the objectives of this approach:

- (i) How is the nonlinear viscoelasticity of the compound affected by changing the rubber grade?
- (ii) How is it affected by changing the carbon black grade?
- (iii) How can we characterise the physical ageing of the compound?

There must be many practical questions of this nature. The proposed approach is the use of strain amplification.

The concept of strain amplification has been around for many years. When a compound is deformed, the matrix must bear a strain larger than that imposed by the macroscopic deformation, because carbon black does not deform. However, establishing a rigorous theory of strain amplification is almost impossible [16] because the microscopic deformation is very different from the macroscopic one. For example, when the macroscopic deformation is elongation, the microscopic deformation includes shear as well as rotation and the spatial rearrangement of fillers. Use of the elongation-equivalent

of strain amplification is proposed here, which includes all the non-elongational contributions described above. Therefore, it is an ‘apparent strain amplification’.

Mullins and Tobin used a simple equation for strain amplification [17], where the apparent amplification is assumed without explicitly stating so. The amplification factor  $\chi$  is

$$\chi = \varepsilon_0/\varepsilon \quad (7.4)$$

where  $\varepsilon_0$  is the matrix strain expressed as the elongation equivalence and  $\varepsilon$  is the observed strain of the compound specimen. If the stress,  $\sigma$ , is uniform throughout, then

$$\chi = E/E_0 \quad (7.5)$$

where  $E$  is the modulus of the compound and  $E_0$  is that of the rubber. In order to evaluate  $\chi$ , the value of  $E_0$  must be known. Mullins and Tobin prepared filled and unfilled vulcanisates with the same crosslinking recipe, through which  $E_0$  was estimated. In order for this method to be valid, the degree of crosslinking for the filled and unfilled rubber must be the same. In general, the presence of carbon black influences the degree of crosslinking [18]. In Equation (7.5),  $E$  and  $E_0$  are equilibrium moduli, so they are functions of strain only. Mullins and Tobin evaluated  $E$  and  $E_0$  from the linear portion at small strains in tensile stress-strain curves. No treatment was given for the strain-dependence of  $\chi$ .

The strain amplification proposed here is very different from that given by Mullins and Tobin. Uncrosslinked rubbers are used and therefore they are not in equilibrium deformation. The material behaviour is time dependent, i.e., viscoelastic. Therefore, the modulus  $E(\varepsilon, \dot{\varepsilon})$  is a function of strain and strain rate,  $\dot{\varepsilon}$ . If the stress is uniform throughout the specimen, Equation (7.5) may be adopted for the dynamic situation. If the matrix is a glass, a stress concentration may occur in the vicinity of fillers. When the matrix is a rubber, the stress concentration dissipates quickly. If the rate of dissipation is much faster than the deformation rate, the stress may be regarded as uniform, and this is the approximation used. At large deformations close to failure, stress concentration may occur and the approximation may not be valid. In such a case the amplification defined by Equation (7.5) includes the effect of the non-uniform stress. The equation is rewritten for the dynamic behaviour as

$$\chi = E_{cp}/E_g \quad (7.6)$$

where  $E_{cp}$  is the compound modulus calculated from the stress ( $\sigma_{cp}$ )-strain ( $\varepsilon_{cp}$ ) measurement, and  $E_g$  is the matrix modulus:

$$E_{cp}(\varepsilon, \dot{\varepsilon}) = \sigma_{cp}/\varepsilon_{cp} \quad (7.7)$$

Likewise the matrix modulus is

$$E_g(\varepsilon, \dot{\varepsilon}) = \sigma_g / \varepsilon_g \quad (7.8)$$

The uniform stress distribution means

$$\sigma_{cp} = \sigma_g \quad (7.9)$$

In Equations (7.7), (7.8) and (7.9) the unknown is  $\varepsilon_g$  and therefore  $E_g$  is also unknown. As it is, Equation (7.6) cannot be solved.

The following method is suggested for the solution. First, a master curve for gum rubber is prepared from the tensile data obtained with several rates of elongation. When the strain-time correspondence is applicable, the master curve gives the relationship [19, 20] :

$$\sigma(\varepsilon, \dot{\varepsilon}) / \varepsilon = E(\alpha t) \quad (7.10)$$

where  $\alpha$  is the extension ratio. When strain-hardening occurs

$$\sigma(\varepsilon, \dot{\varepsilon}) / \varepsilon / \Gamma(\alpha) = E(\alpha t) \quad (7.11)$$

where  $\Gamma(\alpha)$  represents the degree of strain-hardening.

The calculation involves iterative steps; first an arbitrary value is taken for  $\chi$ , e.g.,  $\chi = 3$ . Inserting this value into Equation (7.12):

$$\chi = \varepsilon_g / \varepsilon_{cp} \quad (7.12)$$

$\varepsilon_g$  is obtained as a first approximation  $\varepsilon_{g1}$  for the given value of  $\varepsilon_{cp}$ .

Because

$$\alpha_{g1} = \varepsilon_{g1} + 1 \quad (7.13)$$

and

$$t = \varepsilon_{cp} / \dot{\varepsilon}_{cp} \quad (7.14)$$

$E_{g1}$  can be estimated from the master curve, either Equation (7.10) or (7.11), whichever the case may be. From Equations (7.8) and (7.9):

$$\varepsilon_g = E_g / \sigma_{cp} \quad (7.15)$$

Using  $E_{g1}$  and Equation (7.15), the second approximation  $\varepsilon_{g2}$  is obtained. This completes the first cycle of calculation. The next cycle gives  $\varepsilon_{g3}$ . After repeating the cycle a few times,  $\varepsilon_{gi}$  no longer changes. Then  $\chi$  is calculated from Equation (7.12).

Examples of strain amplification for different gum rubbers with the same formulation (see Table 7.2) are shown in Figures 7.10a and 7.10b [19].

Table 7.2 Diene Rubber Samples						
Type	Trade Mark <sup>a</sup>	Code for gum	Code for compound	Mooney index of gum <sup>b</sup>	% gel of gum	Carbon black, N550 (phr)
NBR	Hycar 1052	A	1	35	0 <sup>c</sup>	40
NBR	Hycar 1042x82	C	3	81	48.6	40
NBR	Hycar 1002	D	4	85	74.3	40
SBR	Ameripol 1502	H	5	52	1.8 <sup>d</sup>	40
SBR	Ameripol 1712	I	7	55	4.4	40 <sup>d</sup>

<sup>a</sup> : Registered trademark of the BFGoodrich Company  
<sup>b</sup> : Reference 4  
<sup>c</sup> : Reference 3  
<sup>d</sup> : A method similar to that of Reference 3 but toluene was used instead of MEK  
<sup>e</sup> : Parts per hundred of gum rubber plus extending oil

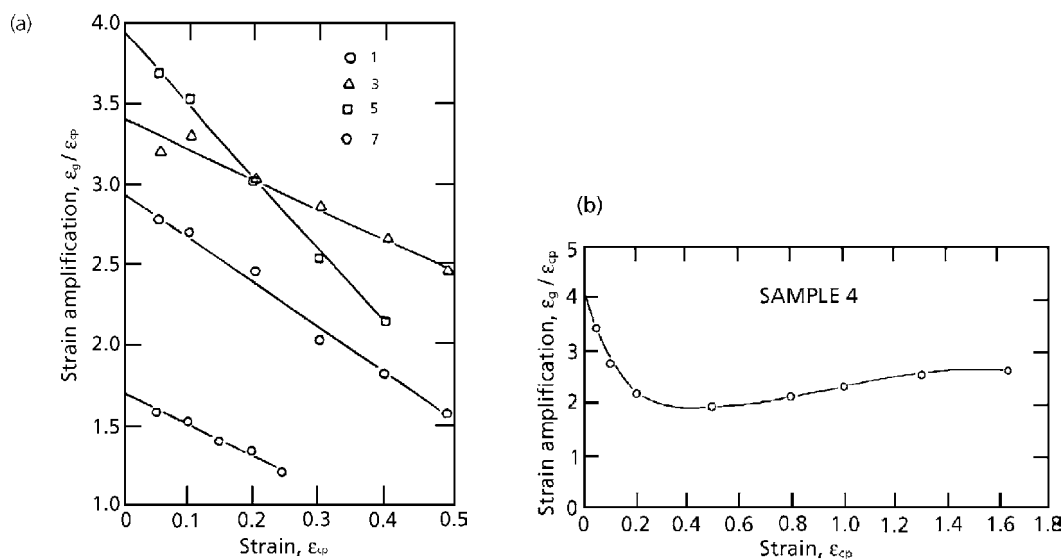


Figure 7.10 a) Strain amplification factor as a function of strain for Samples 1, 3, 5 and 7.  
 b) Strain amplification factor as a function of strain for Sample 4.

Reprinted from N. Nakajima, *Polymer International*, 1996, 40, 2, 141. Copyright 1996, SCI.  
 Reproduced with permission.

As shown in Figure 7.10 the extent of strain amplification varies significantly among the different rubbers. The common trend is a decrease of the amplification with increasing strain. In general, compounds do not elongate much before the yield point is reached; in most cases, less than 50% elongation. Compound 3 contains about 50% microgel [2]. Compound 4 containing 75% macrogel [1] is the only sample giving a large elongation 160%, before yielding. The amplification for Compound 4 decreases up to 20% elongation but thereafter stays about constant. As explained before, the strain amplification arises from multiple sources but may be regarded as the all-inclusive manifestation of rubber-carbon black interaction. For further details the results must be compared with the bound-rubber content, the amount of adsorbed rubber on the carbon black, which may be estimated by nuclear magnetic resonance (NMR) [21, 22, 23], and the extent of development of the secondary network of carbon black (the Payne effect) [10].

Figure 7.11 shows the effect of carbon black grade on the strain amplification [24]. The rubber is ACM having ethylidene norbornene as the cure-site. ACMs in general give a large extension and in this case 500% even as a compound.

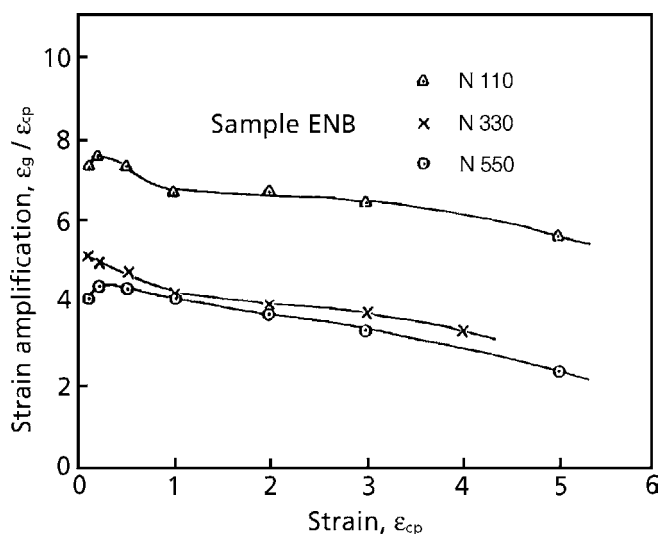


Figure 7.11 Strain amplification of ACM compound ENB, containing 50 phr of carbon black – N110, N330 and N550.

Reprinted from N. Nakajima, *Polymer International*, 1996, 40, 2, 141. Copyright 1996, SCI. Reproduced with permission.

Carbon black N110, which has the smallest particle size of the three, gives the largest strain amplification. Carbon black N330, which has an intermediate particle size, gives a somewhat larger amplification than carbon black N550, having the largest particle size.

When  $\epsilon_g$  is found by this procedure, it may be presented as a function of time (Equation 7.14). From this relationship, the strain rate of the matrix rubber,  $\dot{\epsilon}_g$ , may be estimated. It follows that the strain-rate amplification,  $\dot{\chi}$ , is

$$\dot{\chi} = \dot{\epsilon}_g / \dot{\epsilon}_{cp} \quad (7.16)$$

Figure 7.12 shows the strain-rate amplification calculated from the data of Figure 7.11 [20].

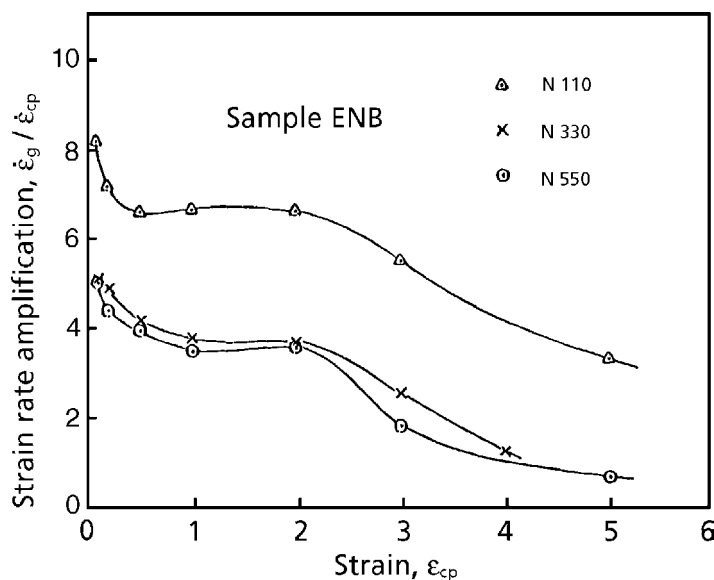


Figure 7.12 Strain-rate amplification of ACM compound ENB, containing 50 phr of carbon black – N110, N330 and N550.

Reprinted from N. Nakajima, *Polymer International*, 1996, 40, 2, 141. Copyright 1996, SCL. Reproduced with permission.

The strain-rate amplification decreases with increasing elongation in two stages. After the initial decrease, the amplification remains constant or increases slightly and then decreases again. At the last point, which is near the yield point, the amplification becomes 1 or even less than 1 with N330 and N550. The strain rate of the matrix is either the

same as, or less than, that of the compound as a whole, suggesting the separation of rubber from the surface of the carbon black.

Figures 7.13 and 7.14 are the strain-amplification and the strain-rate amplification, respectively, of the compounds made with sample EP of ACM. The effect of the particle size of carbon black is the same as that with sample ENB, but the magnitude and the patterns of the amplifications are different between the two gum rubbers.

Figures 7.15 and 7.16 show the effect of the structure of carbon black on the strain amplification. The highest structure, N358, gave the highest amplification but the order is reversed between N330 and N326. This was shown with both samples ENB and EP. The reason for the reversal is not known at this time. Overall, sample ENB gave more pronounced amplification than EP did. This may come from the differences in gel-type and gel-content; ENB containing 70% microgel and EP only 10% macrogel.

Figure 7.17 shows the effect of ageing on the strain amplification [24]. The previous data on the strain amplification (Figure 7.11) were determined within a week after compounding. The aged sample was stored for 2 months. The strain amplification increased almost 50% in 2 months. However, after a slight remilling the original value of the amplification is recovered.

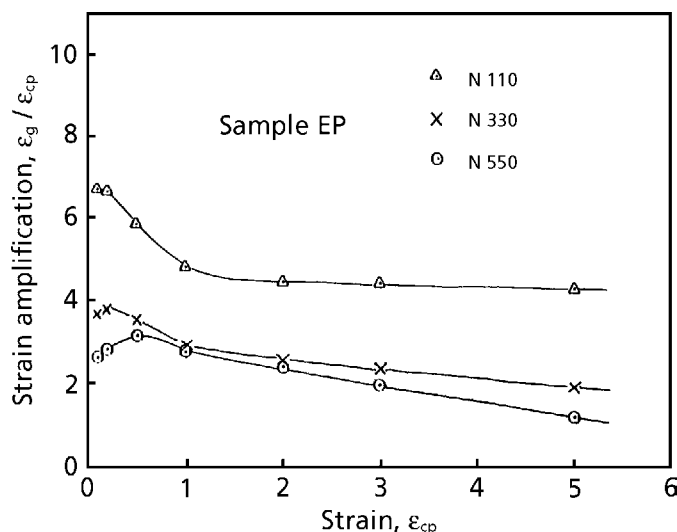


Figure 7.13 Strain amplification of ACM compound EP, containing 50 phr of carbon black – N110, N330 and N550.

Reprinted with permission from N. Nakajima, *Rubber Chemistry and Technology*, 1988, 61, 5, 938. Copyright 1988, Rubber Division of the ACS.



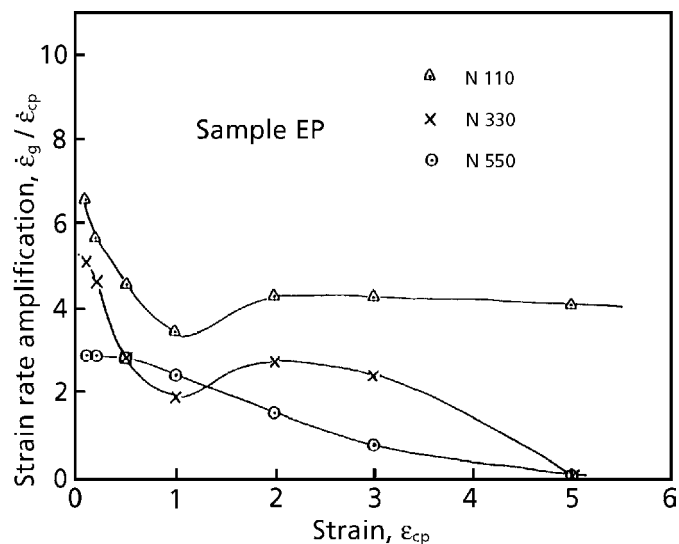


Figure 7.14 Strain-rate amplification of ACM compound EP, containing 50 phr of carbon black – N110, N330 and N550.

Reprinted with permission from N. Nakajima, *Rubber Chemistry and Technology*, 1988, 61, 5, 938. Copyright 1988, Rubber Division of the ACS.

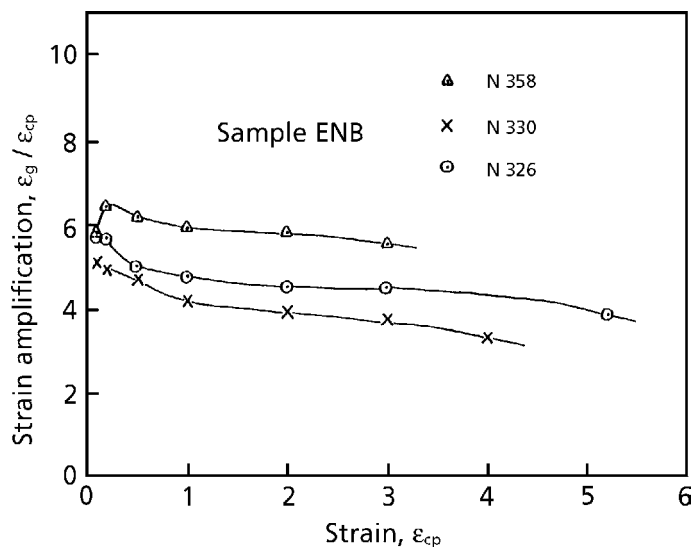


Figure 7.15 Strain amplification of ACM compound ENB, containing 50 phr of carbon black – N358, N330 and N326.

Reprinted with permission from N. Nakajima, *Rubber Chemistry and Technology*, 1988, 61, 5, 938. Copyright 1988, Rubber Division of the ACS.

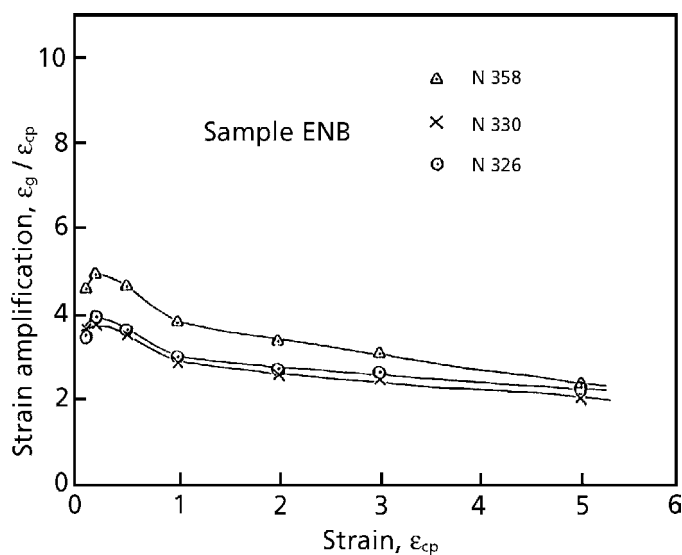


Figure 7.16 Strain amplification of ACM compound EP, containing 50 phr of carbon black – N358, N330 and N326.

Reprinted with permission from N. Nakajima, *Rubber Chemistry and Technology*, 1988, 61, 5, 938. Copyright 1988, Rubber Division of the ACS.

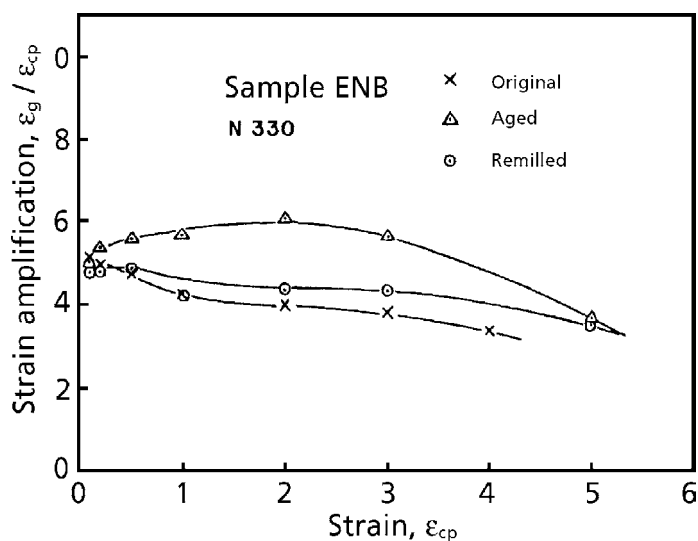


Figure 7.17 Effects of ageing and remilling on strain amplification of ENB compound.

Reprinted from N. Nakajima, *Polymer International*, 1996, 40, 2, 141. Copyright 1996, SCI. Reproduced with permission.

The increase of the compound modulus on ageing may result from an increase of bound rubber and regeneration of entanglement at the interface of the comminuted rubber particles, as discussed in section 4.4 and [24]. Also, a spatial rearrangement of carbon black caused by the memory of the matrix rubber may occur. As the memory recovers very slowly, the compound tends to go back to the previous state, where the dispersion was poorer and the modulus was higher. These three effects may be erased by remilling.

The evaluation of ageing with a Mooney rheometer is not accurate because charging of the specimen erases a part of the ageing. In the strain amplification, a tensile specimen may be stored for ageing and then subjected to the test without loss of the ageing effect.

## **7.4 Unique characteristics of compounds**

The first part of this chapter concerned the viscoelastic properties of gum rubber and how they affect those of the compound. The second part discussed the use of strain amplification as a quantitative measure of the compound characteristics, where the effect of the formulation, i.e., rubber and carbon black variation, were investigated.

There are other qualitative aspects which are unique to rubber compounds and different from gum rubber behaviour. The increase of modulus as a result of physical ageing has already been discussed in section 7.3.

Rubber compounds tend to give a smooth extrudate without melt fracture. Also, the magnitude of the extrudate swell is smaller than that of the gum rubber [5]. Compounds consist of supermolecular flow units, which form during compounding. No fracture occurs at the entrance of the capillary because it is a fluid material. Consequently, the memory of deformation at the entrance is smaller than that of gum rubber, which is an elastic material. This explains the low extrudate swell. The supermolecular flow units are carbon black with adsorbed rubber and comminuted particles of the matrix rubber. There is some resemblance between the rheology of rubber compounds and that of PVC; both are in a particulate state during flow [5].

Compounds tend to slip more easily at the metal-rubber interface compared with gum rubbers. This is observable in extrusion with use of a colour-marker on the specimen [25].

Yielding is observed in elongation of compounds. This occurs at large deformations. The decrease of modulus with increase of the strain amplitude occurs at very small deformations (Payne effect) [9]. This may also be regarded as a yielding of the carbon black network. When the steady state flow measurement is carried to very low shear

rates, the viscosity increases toward infinity [26]. This is interpreted as the manifestation of yield stress. All these yieldings are not the same kind; nevertheless they are unique to compounds and do not occur with gum rubbers. These aspects will be discussed in Chapter 8.

## **7.5 Application of characterisation methods for a specific problem**

In section 7.2 it was shown that the differences in the viscoelastic behaviour among gum rubbers are carried into the differences among corresponding rubber compounds. The observation is semi-quantitative but it is important to demonstrate the trend.

In section 7.3 a quantitative relationship between a gum rubber and its compound in the elongational behaviour is described in terms of strain- and strain-rate amplification. The variables are

- (a) differences among the matrix rubbers with the same filler
- (b) differences among fillers in the same matrix rubber
- (c) differences in aged and unaged compound.

In this section even more detailed questions are asked about the specific effect of branching and that of crystalline particle fillers in gum rubbers on the elongational behaviour of compounds. The filler type is also a variable. A quantitative comparison is intended in this section [27].

### **7.5.1 Effect of fillers and rubber structures on tensile behaviour of filled, unvulcanised compounds of *cis*-1,4-polybutadiene**

- *Experiment*
- *Sample*

Samples of gum rubbers and fillers used for the compounds are listed in Table 7.3. These gum rubbers were chosen from eight previously studied samples, which represented three different groups. These groups were titanium-, neodymium-, and cobalt-polymerised polymers. The titanium-polymerised CB11 had a higher degree of branching but the branches were relatively short, causing strain softening. Neodymium-polymerised CB22 had a lower degree of branching than CB11, but the branches were relatively long and exhibited strain hardening. The cobalt-polymerised VCR 412 contained 12% crystalline

particles made from a block copolymer of *cis*-1,4- and 1,2-polybutadiene [28]. The particles produced strain softening. The *cis*-1,4-branches attached to the surface of the particles were relatively short and facilitated the elongation.

Table 7.3 Samples				
Sample Designation	Catalyst Type	<i>cis</i> Content	Mooney Index of gum	Filler Loading (phr)
BUNA <sup>a</sup> CB11	Ti	<i>cis</i> -BR, 93%	47	N110 <sup>b</sup> 50 N330 <sup>b</sup> 50
BUNA <sup>a</sup> CB22	Nd	<i>cis</i> -BR, 98%	63	N110 <sup>b</sup> 50 N330 <sup>b</sup> 50 VN3 <sup>c</sup> 56 VN3 <sup>c</sup> 56 Si 69 <sup>d</sup> 5.6
VCR <sup>e</sup> 412	Co	<i>cis</i> -BR, 91% and SPB <sup>f</sup>	45	N110 <sup>b</sup> 50 N330 <sup>b</sup> 50
<sup>a</sup> : Registered trademark of Bayer AG <sup>b</sup> : Produced by Cabot <sup>c</sup> : Silica produced by Degussa <sup>d</sup> : Bis(3-[triethoxysilyl]propyl)tetrasulphane-coupling agent produced by Degussa <sup>e</sup> : Registered trademark of UBE Industry <sup>f</sup> : Crystalline particles made of block copolymer of <i>cis</i> -1,4- and syn-1,2-polybutadiene				

The amount of silica was adjusted to make its volume equal to the volume of 50 phr carbon black by taking account of the density difference.

- *Mixing*

A Banbury-type internal mixer with a 250 ml capacity was used. The fill factor was 0.7 and the rotor speed was 100 rpm. First the mixer was cleaned with gum rubber.

Then, fresh rubber was charged and masticated for 1 minute. At this time half of the carbon black was added over a period of 1 minute. After an additional 30 seconds of mixing the rest of the carbon black was added. After mixing for another 2 minutes, the compound was dumped. For mixing silica, one-third was added every minute. After an additional 4 minutes of mixing the compound was dumped. The coupling agent was added with the second addition of silica. All dumped compounds were crumbly and a small amount of the free filler remained.

The dumped compounds were milled and sheeted with a 6-inch two roll mill to develop further mixing and to observe mill behaviour of the compounds. All compounds were pressed at 140 °C for 10 minutes for preparation of tensile specimens.

- *Tensile measurement*

Tensile measurements were performed with a Monsanto Tensometer 500. The strip chart recorder recorded force against time. The force was measured with a 45 kg load cell. The extent of deformation was measured by recording with a video camera. The measurements were performed at room temperature with deformation rates of 0.035, 0.082, and 0.176 s<sup>-1</sup>.

- *Results and discussion*

Examples of stress-strain curves at various deformation rates are shown in Figures 7.18-7.21 where the stress is the true stress, assuming incompressibility of the compounds.

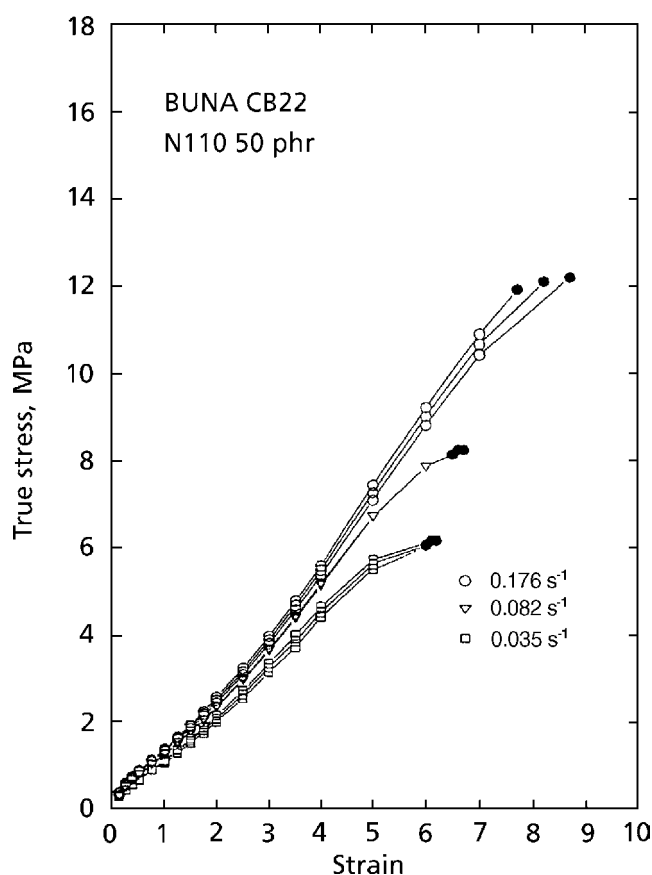


Figure 7.18 Tensile stress-strain curves of CB22 compound with carbon black N110.

*Reprinted from N. Nakajima and Y. Yamaguchi, Journal of Applied Polymer Science, 1997, 66, 8, 1445. Copyright 1997, reprinted by permission of John Wiley & Sons, Inc.*

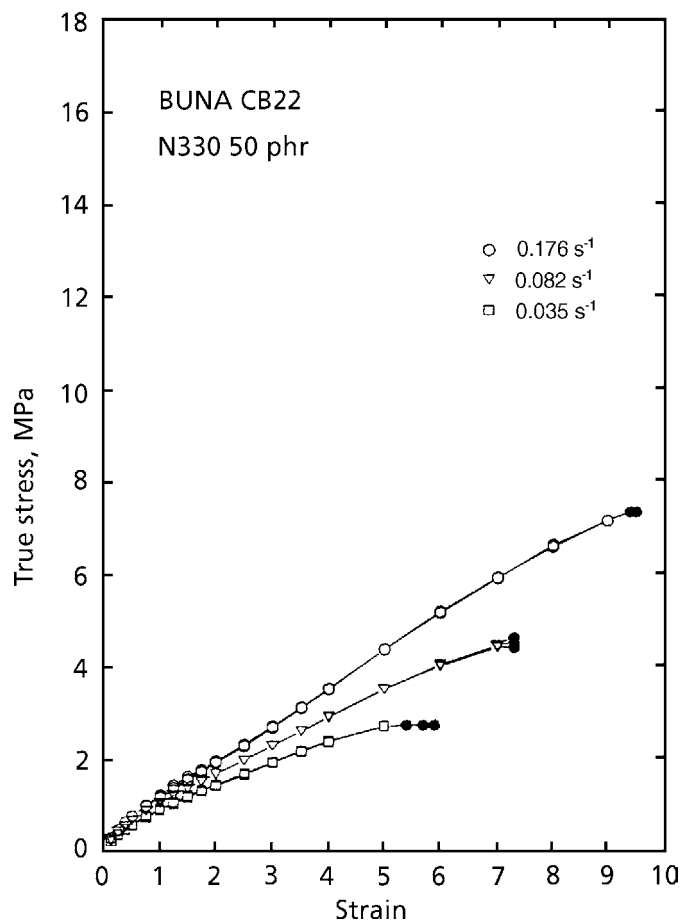


Figure 7.19 Tensile stress-strain curves of CB22 compound with carbon black N330.

Reprinted from N. Nakajima and Y. Yamaguchi, *Journal of Applied Polymer Science*, 1997, 66, 8, 1445. Copyright 1997, reprinted by permission of John Wiley & Sons, Inc.

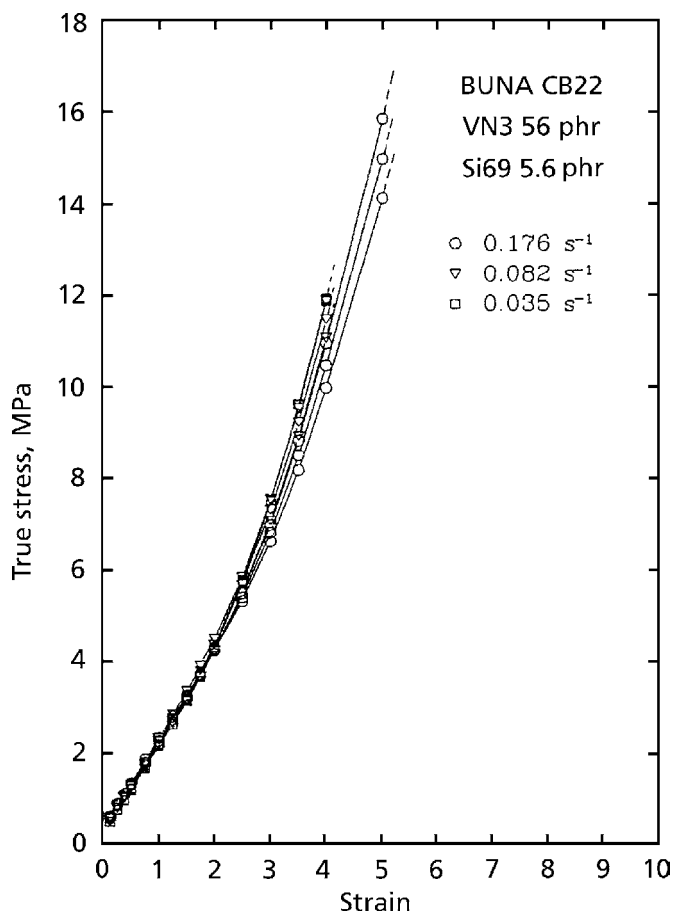


Figure 7.20 Tensile stress-strain curves of CB22 compound with silica and coupling agent.

Reprinted from N. Nakajima and Y. Yamaguchi, *Journal of Applied Polymer Science*, 1997, 66, 8, 1445. Copyright 1997, reprinted by permission of John Wiley & Sons, Inc.



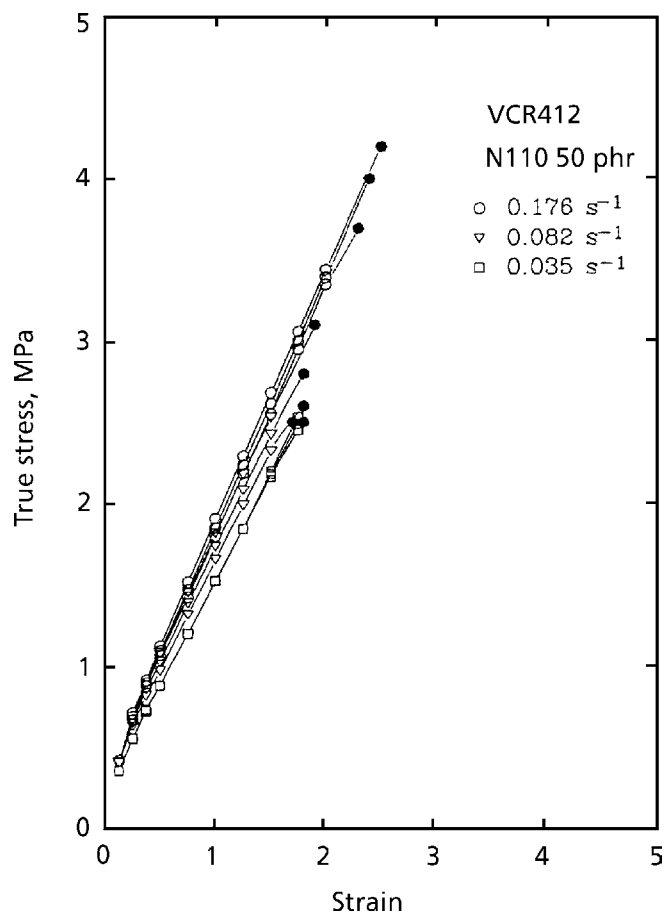


Figure 7.21 Tensile stress-strain curves of VCR412 compound with carbon black N110.

Reprinted from N. Nakajima and Y. Yamaguchi, *Journal of Applied Polymer Science*, 1997, 66, 8, 1445. Copyright 1997, reprinted by permission of John Wiley & Sons, Inc.

The data with the same symbol shows reproducibility of the measurement, which was within  $\pm 3\%$ . It was smaller compared to that of the gum rubbers,  $\pm 15\%$ . The stress-strain curves of the carbon black compounds include failure data shown by filled circles. The silica-filled compound of CB22 with coupling agent was very stiff and the specimen slipped out of the grips at the high elongation. With this compound the stress decreased slightly with the increasing deformation rate at the large deformation. This may be the error resulting from slipping. However, the silica-filled compound without the coupling agent and the carbon black filled compounds showed the increase of stress with increasing deformation rate.

In Figures 7.22-7.24, stress-strain curves of gum rubbers and their filled compounds are compared.

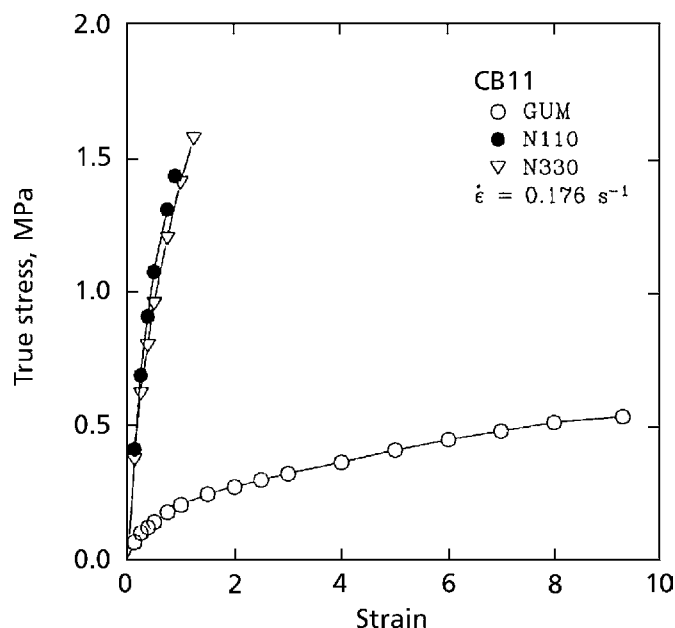


Figure 7.22 Comparison of tensile stress-strain curves of gum rubber and compounds of CB11.

Reprinted from N. Nakajima and Y. Yamaguchi, *Journal of Applied Polymer Science*, 1997, 66, 8, 1445. Copyright 1997, reprinted by permission of John Wiley & Sons, Inc.

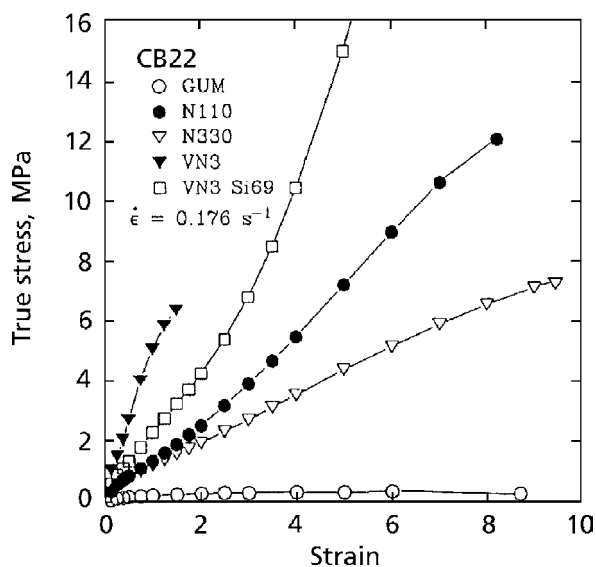


Figure 7.23 Comparison of tensile stress-strain curves of gum rubber and compounds of CB22.

Reprinted from N. Nakajima and Y. Yamaguchi, *Journal of Applied Polymer Science*, 1997, 66, 8, 1445. Copyright 1997, reprinted by permission of John Wiley & Sons, Inc.

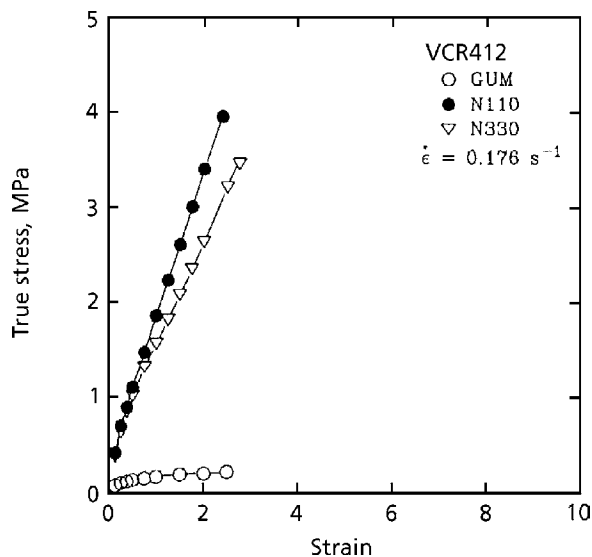


Figure 7.24 Comparison of tensile stress-strain curves of gum rubber and compounds of VCR412.

Reprinted from N. Nakajima and Y. Yamaguchi, *Journal of Applied Polymer Science*, 1997, 66, 8, 1445. Copyright 1997, reprinted by permission of John Wiley & Sons, Inc.

The stresses for all the compounds are greatly increased by the filler. The gum rubbers of CB11 and CB22 showed a similar elongation at break. However, the elongation at break of the CB11 compound was considerably reduced in the presence of carbon black whereas that of the CB22 compound was unaltered. From previous work [29], CB11 was known to have a higher degree of branching than CB22, but the branches of the former were found to be relatively short whereas those of the latter were long. The more branched rubber is generally known to have a higher affinity to carbon black. This together with the shortness of the branches may be the cause of the reduced elongation at break of the CB11 compound.

On the other hand, long branches are known to aid the retention of elongation at break upon loading with carbon black [19]. This fact accounts for the behaviour of the CB22 compound.

Gum VCR 412 has a much lower strain at break compared to CB11 and CB22. The matrix rubber of VCR 412 is not significantly different from that of CB22, except that it contains crystalline particles. Therefore, the crystalline particles must be affecting the decrease of strain at break. The addition of carbon black does not decrease the strain at break. In this respect it is similar to the CB22.

Referring to Figure 7.23, the silica-filled compound without the coupling agent shows the highest modulus. This is because of the poor dispersion of the filler [30]. The compound with silica and the coupling agent show lower modulus because of a better dispersion. This compound behaves like a crosslinked network; the stress rise indicates limited extensibility. The coupling agent is known to give premature crosslinking during compounding [31]. The carbon black filled compounds show lower modulus than those of silica-filled compounds because of the better dispersion. The compounds with smaller particles of carbon black (N110) show higher modulus than that with larger particles (N330); the better reinforcement from smaller particles is well recognised.

Figures 7.25 and 7.26 show modulus as a function of reduced time (Equation 6.27).

The lines connect the data at the same strain and parallel lines at different strains were obtained. Master curves after application of the modulus shift, Equation. 6.29, are shown in Figures 7.27 and 7.28.

With all compounds the master curves were obtained after the time and the modulus shift. As shown in Figures 7.29-7.31, the direction of the modulus shift was that of strain softening for all compounds.

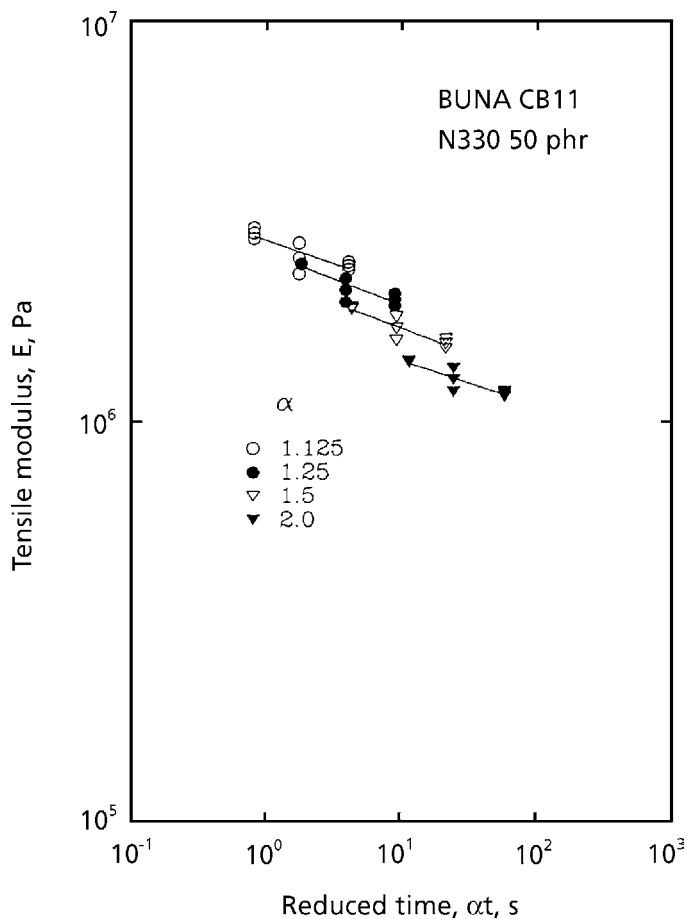


Figure 7.25 Tensile modulus as a function of reduced time at fixed extension ratios for CB11.

*Reprinted from N. Nakajima and Y. Yamaguchi, Journal of Applied Polymer Science, 1997, 66, 8, 1445. Copyright 1997, reprinted by permission of John Wiley & Sons, Inc.*

The different behaviour of gum rubbers CB11 and CB22 (i.e., strain softening versus strain hardening [29]) is apparently carried over to the difference in the behaviour of the corresponding compounds; that is, the initial strain softening of the CB11 compounds is much higher than that of the CB22 compounds. Also, the softening trends were reversed at the higher elongation in the CB22 compounds (Figure 7.30), indicating the strain hardening of the matrix rubber.

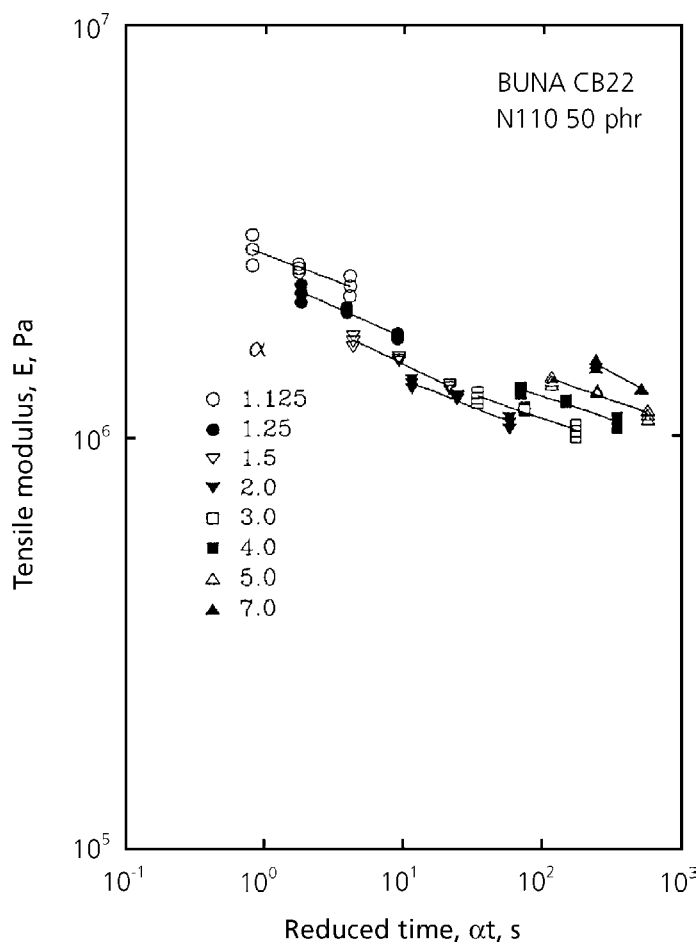


Figure 7.26 Tensile modulus as a function of reduced time at fixed extension ratios for CB22.

Reprinted from N. Nakajima and Y. Yamaguchi, *Journal of Applied Polymer Science*, 1997, 66, 8, 1445. Copyright 1997, reprinted by permission of John Wiley & Sons, Inc.

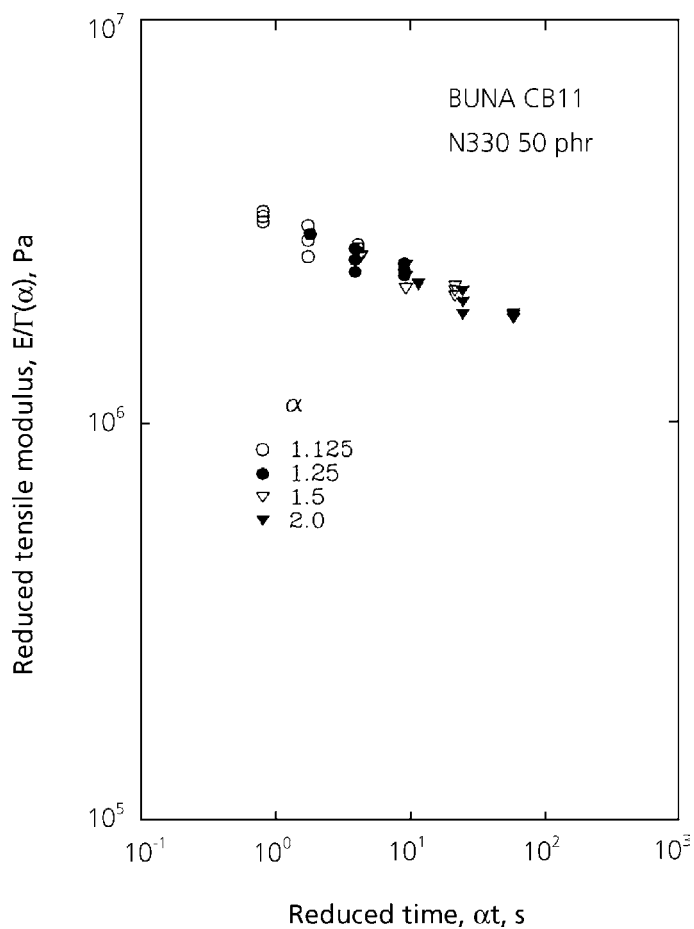


Figure 7.27 Reduced tensile modulus as a function of reduced time at fixed extension ratios for CB11.

Reprinted from N. Nakajima and Y. Yamaguchi, *Journal of Applied Polymer Science*, 1997, 66, 8, 1445. Copyright 1997, reprinted by permission of John Wiley & Sons, Inc.

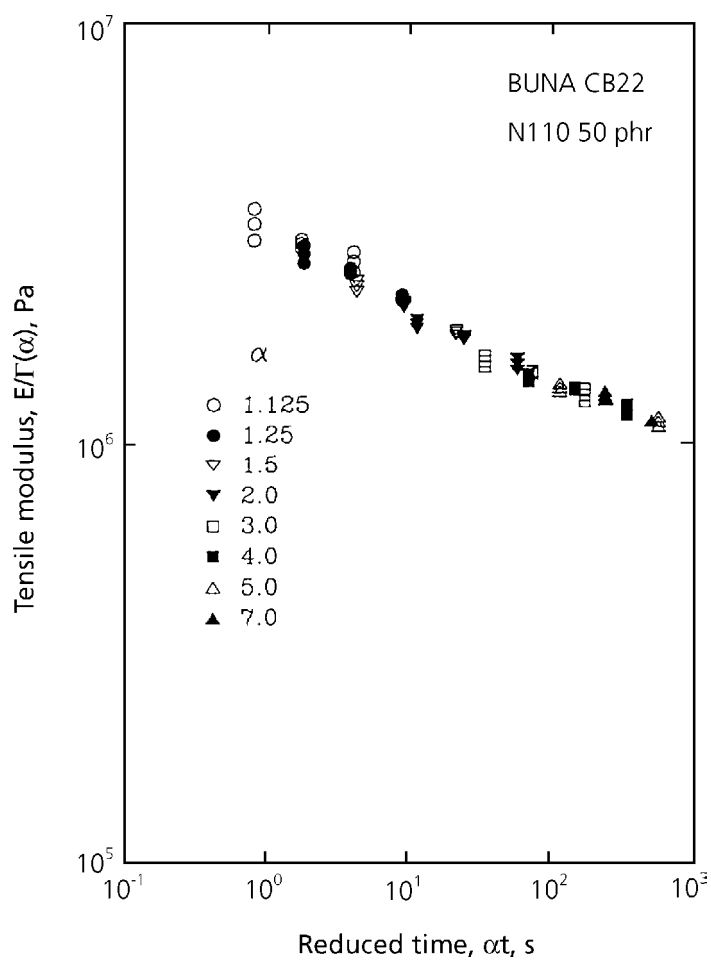


Figure 7.28 Reduced tensile modulus as a function of reduced time at fixed extension ratios for CB22.

Reprinted from N. Nakajima and Y. Yamaguchi, *Journal of Applied Polymer Science*, 1997, 66, 8, 1445. Copyright 1997, reprinted by permission of John Wiley & Sons, Inc.



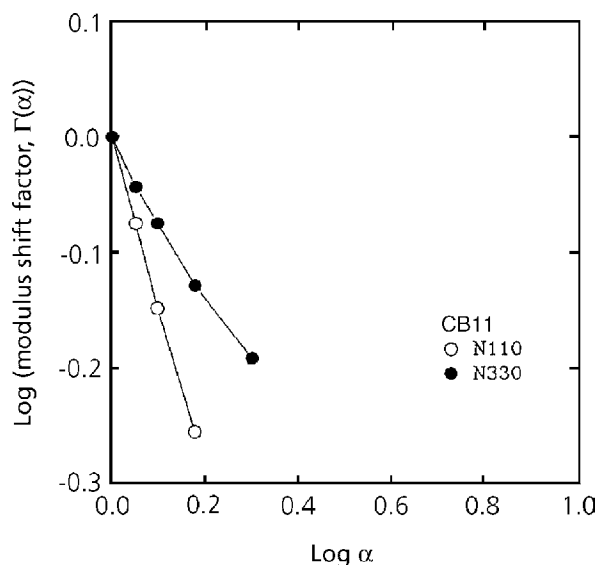


Figure 7.29 Modulus shift factors as a function of extension ratio for CB11 compounds indicating degree of strain softening.

Reprinted from N. Nakajima and Y. Yamaguchi, *Journal of Applied Polymer Science*, 1997, 66, 8, 1445. Copyright 1997, reprinted by permission of John Wiley & Sons, Inc.

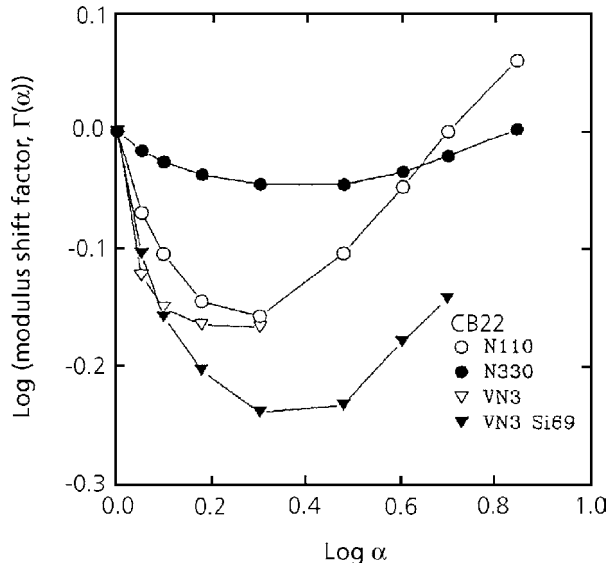


Figure 7.30 Modulus shift factors as a function of extension ratio for CB22 compounds indicating degree of strain softening.

Reprinted from N. Nakajima and Y. Yamaguchi, *Journal of Applied Polymer Science*, 1997, 66, 8, 1445. Copyright 1997, reprinted by permission of John Wiley & Sons, Inc.

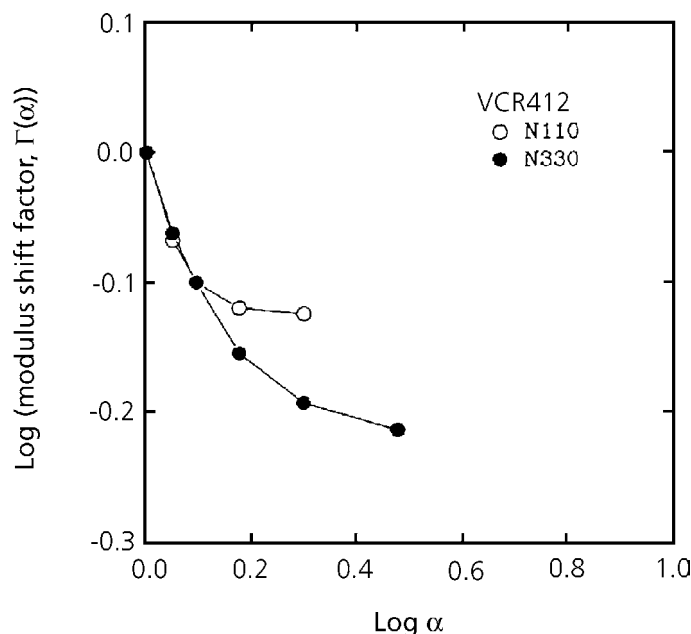


Figure 7.31 Modulus shift factors as a function of extension ratio for VCR412 compounds indicating a degree of strain softening.

Reprinted from N. Nakajima and Y. Yamaguchi, *Journal of Applied Polymer Science*, 1997, 66, 8, 1445. Copyright 1997, reprinted by permission of John Wiley & Sons, Inc.

The N110 filled compounds of CB11 and CB22 show large degrees of strain-softening compared to those filled with N330 compounds. On the other hand VCR412 compounds with N110 and N330 behave similarly. The carbon black N110 is more difficult to disperse than the N330. The compounds exhibiting a greater degree of strain softening, when other variables are unchanged, have relatively poor dispersion of the filler. VCR412 was the easiest to handle on the mill when either of the carbon blacks was incorporated. This accounts for the same degree of strain softening for N110 and N330. On the other hand, if we compare CB22 and VCR412 compounds with carbon black N330 (see Figures 7.30, and 7.31), the CB22 compound shows much less strain softening than the VCR412 compound does. The difference must come from the difference of the behaviours of the matrix rubbers: CB22 produces strain hardening and VCR412 strain softening. These rubbers with N110 show the same degree of strain softening. As mentioned, the explanation is a poor dispersion of N110 in CB22, a fact that resulted in substantial strain softening.

The effect of silica on strain softening is larger than that of carbon black. This is because of the poorer dispersion of silica compared to that of carbon black. Because of the poor dispersion of the silica and anomalous crosslinking due to the coupling agent, no further comment can be made for the silica-filled compounds.

Whereas the extent and the manner of the strain softening provides useful information on the effects of fillers and that of the structure of matrix rubbers, the data are taken relative to the moduli at the infinitesimal strain. Therefore, the absolute magnitude of moduli must also be examined. The data in Table 7.4 indicate clearly that the moduli of CB22 compounds are significantly lower than those of CB11 and VCR412 at all strain rates. In the previous observations [29, 32] with gum rubbers, CB22 did not give a noticeable strain-induced crystallisation while CB11 and VCR412 clearly indicated crystallisation. Therefore, the above differences in the compound moduli are attributable to the difference in the ease of strain-induced crystallisation of the matrix rubbers.

Table 7.4 Tensile Modulus of Compound									
	CB11			CB22			VCR412		
	M50	M100	M200	M50	M100	M200	M50	M100	M200
$\dot{\epsilon}=0.176 \text{ s}^{-1}$									
N110	1.08	–	–	0.85	1.34	2.48	1.10	1.86	3.40
N330	0.96	1.41	–	0.76	1.19	1.93	1.01	1.57	2.64
$\dot{\epsilon}=0.082 \text{ s}^{-1}$									
N110	1.03	–	–	0.77	1.24	2.33	1.03	1.74	–
N330	0.85	1.27	–	0.66	1.05	1.67	0.87	1.36	2.36
$\dot{\epsilon}=0.035 \text{ s}^{-1}$									
N110	0.92	–	–	0.66	1.08	2.06	0.89	1.53	–
N330	0.88	1.18	–	0.57	0.91	1.43	0.82	1.33	2.27
M50, M100 and M200 are the modulus at 50, 100 and 200% strain, respectively									

## References

1. N. Nakajima, H. H. Bowerman and E. A. Collins, *Journal of Applied Polymer Science*, 1977, **21**, 11, 3063.
2. N. Nakajima, *Polymer International*, 1995, **36**, 2, 105.
3. ASTM D3616-95  
*Standard Test Method for Rubber, Raw - Determination of Gel, Swelling Index and Dilute Solution Viscosity.*
4. ASTM D1646-96a  
*Standard Test Methods for Rubber - Viscosity, Stress Relaxation and Pre-Vulcanization Characteristics (Mooney Viscometer).*
5. N. Nakajima and E. A. Collins, *Rubber Chemistry and Technology*, 1975, **48**, 4, 615.
6. T. L. Smith in *Rheology: Theory and Applications*, Volume 5, Ed., F. R. Eirich, Academic Press, New York, 1969, Chapter 4
7. N. Nakajima, *Polymer Engineering and Science*, 1979, **19**, 3, 215.
8. W. P. Cox and E. H. Merz, *Journal of Polymer Science*, 1958, **28**, 118, 619.
9. A. R. Payne and R. E. Whittaker, *Rubber Chemistry and Technology*, 1971, **44**, 2, 440.
10. *Reinforcement of Elastomers*, Ed., G. Kraus, Wiley, New York, 1965, Chapter 3.
11. A. K. Sircar and A. Voet, *Rubber Chemistry and Technology*, 1970, **43**, 5, 973.
12. N. Nakajima, J. J. Scobbo, Jr., and E. R. Harrell, *Rubber Chemistry and Technology*, 1987, **60**, 5, 761.
13. N. Nakajima, *Journal of Non-Newtonian Fluid Mechanics*, 1983, **12**, 349.
14. S. Montes, J. L. White and N. Nakajima, *Journal of Non-Newtonian Fluid Mechanics*, 1988, **28**, 183.
15. N. Nakajima and E. R. Harrell, in *Encyclopedia of Fluid Mechanics*, Volume 9, Ed., N. P. Cheremisinoff, Gulf Publishing Co., Houston Texas, 1990, p.277-314.
16. F. Bueche in *Reinforcement of Elastomers*, Ed., G. Kraus. Wiley, New York, 1965, p.6.

17. L. Mullins and N. R. Tobin, *Rubber Chemistry and Technology*, 1967, **39**, 4, 799.
18. G. Kraus in *Science and Technology of Rubber*, Ed., F. R. Eirich, Academic Press, New York, 1978, p.339.
19. N. Nakajima and J. J. Scobbo, Jr., *Rubber Chemistry and Technology*, 1988, **61**, 1, 137.
20. N. Nakajima, *Rubber Chemistry and Technology*, 1988, **61**, 5, 938.
21. H. Serizawa, M. Ito, T. Kanamoto, K. Tanaka and A. Nomura, *Polymer Journal (Japan)*, 1982, **14**, 2, 149.
22. H. Serizawa, T. Nakamura, M. Ito, K. Tanaka and A. Nomura, *Polymer Journal (Japan)*, 1983, **15**, 3, 201.
23. H. Serizawa, T. Nakamura, M. Ito, K. Tanaka and A. Nomura, *Polymer Journal (Japan)*, 1983, **15**, 3, 543.
24. N. Nakajima and R. A. Miller, *Rubber Chemistry and Technology*, 1988, **61**, 2, 362.
25. C. Y. Ma, J. L. White, F. C. Weissert, A. I. Isayev, N. Nakajima and K. Min, *Rubber Chemistry and Technology*, 1985, **58**, 4, 815.
26. H. J. Song, J. L. White, K. Min, N. Nakajima and F. C. Weissert, *Advances in Polymer Technology*, 1988, **8**, 4, 431.
27. N. Nakajima and Y. Yamaguchi, *Journal of Applied Polymer Science*, 1997, **66**, 8, 1445.
28. M. Takayanagi, Presented at the 19th Annual Meeting of the International Institute of Synthetic Rubber Producers, Hong Kong, 1978, Paper No.21.
29. N. Nakajima and Y. Yamaguchi, *Journal of Applied Polymer Science*, 1996, **61**, 9, 1525.
30. M. P. Wagner, *Rubber Chemistry and Technology*, 1976, **49**, 3, 703.
31. N. Nakajima, W. J. Shieh and Z. G. Wang, *International Polymer Processing*, 1991, **6**, 4, 290.
32. N. Nakajima and Y. Yamaguchi, *Journal of Applied Polymer Science*, 1996, **62**, 13, 2329.

